SANS Study of Sulfonate End Group Effect on Polystyrene Self-Diffusion

S. D. Kim,[†,‡,§,||] A. Klein,[†,‡,⊥,#] and L. H. Sperling*[,†,‡,§,#,▽]

Center for Polymer Science and Engineering, Polymer Interfaces Center, Materials Research Center, Department of Physics, Emulsion Polymers Institute, Department of Chemical Engineering, Department of Materials Science and Engineering, Lehigh University, Bethlehem, Pennsylvania 18015-3194

E. M. Boczar

Rohm and Haas Company, 727 Norristown Rd, Spring House, Pennsylvania 19477

B. J. Bauer

Polymer Division, National Institute of Standards and Technology, Gaithersburg, Maryland 20899

Received March 9, 2000

ABSTRACT: Film formation from a latex involves interdiffusion of polymer chains. The interdiffusion behavior of polystyrene with H ends, one sulfonate end, and two sulfonate ends are compared via small-angle neutron scattering (SANS) and a direct nonradiative energy transfer technique (DET) at short times. High molecular weight ($M_n \cong 300\,000$) anionically synthesized polystyrenes were confined in latex particles utilizing an artificial miniemulsification technique. Interdiffusion of the polystyrenes in a latex film was carried out at temperatures of 125−145 °C. The diffusion coefficients of polystyrene with H ends were five times and 10 times higher than that of polystyrene with one sulfonate end and two sulfonate ends, respectively. The probable cause is end-to-end aggregation of the chains, supported by the ratio $R_g/M^{1/2}$ remaining substantially constant.

Introduction

In the present study, polystyrene interdiffusion from miniemulsified latices was investigated using SANS and DET, examining the effect of sulfonate end groups located at the water/polymer latex interfaces. Emphasis was placed on interdiffusion at short times, in the $t^{1/4}$ regime.

The influence of polymer chain end groups on interdiffusion is of special interest due to the differences in their behavior compared to the central portions of the chain.[1] According to reptation theory, polymer chain ends play a significant role in polymer diffusion processes because they *lead* the main chain out of their virtual tubes. In industrial practice, polymer chain ends may have various chemical structures depending on the use of initiators, chain transfer agents, or other special chemistries.

The location of polymer end groups at interfaces has been studied experimentally[2−6] and theoretically.[7−10] Even in the absence of specific interactions between mers and an interface, the chain ends tends to be segregated at interfaces in order to lower the free energy of the interface. In the case where there are specific interactions, however, important effects of the end groups on surface segregation have been found.[6,11] Elman et al.[6] studied chain-end segregation with neutral, attractive, and repulsive end group systems. The concentration of end groups at an air-repulsive carboxyl group system was depleted at an air interface, while the end group concentration in systems with air-attractive fluorocarbon chain ends was found to be higher at the surface than in the bulk.

The examples cited above were for systems under equilibrium conditions, with the samples being annealed above T_g. However, there are important cases where the polymer surface is not in an equilibrium state. For example, a cracked surface may have a high concentration of chain ends due to chain scission. The chain ends remain at the surface unless the surface is annealed. This nonequilibrium state of having a higher number of chain ends at the surface induces faster crack healing rates than am annealed surface,[12] due to a more rapid interdiffusion.

Another practical example of a nonequilibrium system involves latex particles. It is well-known that sulfate end groups of polymer chains are likely to be on the latex particle surface due to their ionic nature.[13] During the film forming process, interfaces change from polymer/water to polymer/polymer. Therefore, the end groups segregated on the particle surfaces as initially quenched in nonequilibrium states become exposed to other polymer particles on contact.

Yoo and co-workers[14,15] and Kim and co-workers[16] investigated latex film formation by SANS methods to understand the interdiffusion process. They measured diffusion coefficients in both anionically polymerized and free-radical polymerized polystyrene. The diffusion coefficients of latex films from conventional emulsion systems[14,15] were an order of magnitude slower than those observed in the anionic miniemulsification system. The apparent slow interdiffusion in the conventional

[†] Center for Polymer Science and Engineering, Lehigh University.
[‡] Polymer Interfaces Center, Lehigh University.
[§] Materials Research Center, Lehigh University.
[||] Department of Physics, Lehigh University.
[⊥] Emulsion Polymers Institute, Lehigh University.
[#] Department of Chemical Engineering, Lehigh University.
[▽] Department of Materials Science and Engineering, Lehigh University.

10.1021/ma000432u CCC: $19.00
Published on Web 10/07/2000

system was attributed to sulfate end group and/or to a broad molecular weight distribution where the shortest chains interdiffused before measurements began.

Kim and Winnik[17] used a DET technique to investigate interdiffusion in poly(butyl methacrylate) latex films made by conventional emulsion polymerization, comparing neutralized and protonated sulfate end groups. The results of this work indicate that the protonated sulfate end groups induced faster interdiffusion than those in the salt form.

Interdiffusion at short-times is of special interest because most changes in crack healing processes, molding, and latex film formation all occur during this time regime. For example, the mechanical strength in a latex film approaches its maximum when the interdiffusion distance is equal to about one-half radius of gyration, typically less than a few tens of nanometers for most commercial polymers.[14,16] Confirming theory,[12] experimental data has shown that at short times, the strength of interfaces depends on annealing time to the one-fourth power during crack healing,[18] polymer welding,[19] and latex film formation.[16]

Theory

Diffusion of a freely moving polymer molecule can be divided into different time scales. At a very short time scale, local motion such as rotation and vibration dominates, while even at longer times, such motions do not contribute to center-of-mass movement. Because of the large size of a polymer chain, most local motion has a relatively long relaxation time which can be measured easily. At longer times, the Fickian diffusion model describes the center of mass motion.

The de Gennes reptation theory[20,21] describes diffusion among entangled polymer chains. In this model, the chain moves like a snake in an imaginary tube consisting of neighboring polymer chains. The lateral motion of a chain is very restricted, and the polymer chain ends lead the polymer chain during the diffusion processes. Using scaling concepts, de Gennes found that the diffusion coefficient, D, and the relaxation time, T_r, depend on the molecular mass, M, as

$$D \sim M^{-2} \tag{1}$$

$$T_r \sim M^{-3} \tag{2}$$

On the basis of de Gennes' theory, Kim and Wool[22] developed a minor chain reptation model to describe the motion of the polymer chains at interfaces. The average chain interpenetration depth, $d(t)$, was found to scale as follows:

$$d(t) \sim t^{0.25} M^{-0.25} \qquad t < T_r \tag{3}$$

$$d(t) \sim t^{0.5} M^{-1} \qquad t < T_r \tag{4}$$

The interpenetration depth equals the radius of gyration of the polymer chain at $t = T_r$.

Small-Angle Neutron Scattering (SANS)

For SANS measurements, a latex film is composed of both protonated and deuterated types of particles. Scattered neutrons arising from the differences in scattering lengths show different intensities as a function of the scattering angle. The size of the deuterated particles is calculated by a Guinier plot using

$$I(Q) = I(0) \exp\left(-\frac{Q^2 R_g^2}{3}\right) \tag{5}$$

where $I(Q)$ constitutes the probability that a neutron will be scattered in a unit solid angle, per volume of the material (in units of cm^{-1}), characterized by the angle function Q. The wave vector, Q, equals $(4\pi/\lambda)\sin(\theta/2)$, where λ and θ represent the neutron wavelength and the angle between the incident and the scattered beam, respectively.

The radius of a sphere, R, can be calculated from the radius of gyration:

$$R^2 = \frac{5}{3} R_g^2 \tag{6}$$

Equation 6 was also used to express the apparent particle radius increase during diffusion, although the equation is strictly valid only for solid spherical particles with uniform interiors. The apparent size of a particle increases as polymer chains diffuse out across the original particle boundaries. The interpenetration depth, $d(t)$, of polymer chains across the particle boundaries is defined[14] by the difference in particle radius between the particle size at time t, $R(t)$, and the initial particle radius, R_o.

$$d(t) = R(t) - R_o \tag{7}$$

Summerfield and Ullman[23] derived an equation to extract the polymer self-diffusion coefficients from SANS data in deuterated/protonated latex blends. A more general equation based on their work was developed to extend the applicability of the equation[24]

$$I(Q,t) = I(Q,0)\exp(-2Q^2Dt) + I(Q,\infty)[a(t) - a(0)\exp(-2Q^2Dt)] \tag{8}$$

where $I(Q,t)$ represents the scattering intensity at time t and wave vector Q, and $a(t)$ provides a fractional measure of the extent of intermixing during the interdiffusion process. When the diffusion time is small and the wave vector Q is small, $I(Q,\infty)$ is much smaller than $I(Q,t)$ and eq 8 reduces to

$$I(Q,t) = I(Q,0)\exp(-2Q^2Dt) \tag{9}$$

Combination of eqs 5 and 9 provides another way to calculate the diffusion coefficient, D:

$$R_g^2(t) = R_g^2(t_o) + 6D(t - t_o) \tag{10}$$

Equation 10 assumes the diffusion process is Fickian, as do eqs 8 and 9. Also, the scattering intensity at zero angle, $I(0,t)$ remains constant as a function of annealing at early times because the deuterated polymer content of the samples remains the same.

An ideal two-phase system with sharp interfaces has been treated by Porod, who predicted a decrease in intensity proportional to Q^{-4}:

$$I(Q) = \frac{K_p}{Q^4} \tag{11}$$

where K_p is the so-called Porod constant. The deviation

Table 1. Molecular Weights by GPC and the Functionality of SO_3 End Groups

designation	sample	M_n[a] (nominal)	M_w/M_n	M_n[b] (measured)	f[c]
h-H	H-ends (protonated)	327 300	1.05		
d-H	H-ends (deuterated)	320 300	1.05	318 900	
h-P	one SO_3 end (protonated)	318 700	1.09		0.98
d-P	one SO_3 end (deuterated)	315 400	1.09	268 600	0.94
h-S	two SO_3 ends (protonated)	317 000	1.11		1.90
d-S	two SO_3 ends (deuterated)	339 200	1.11	252 600	1.88

[a] Determined by Polymer Source, Inc. [b] By Waters GPC with three columns (Waters Styrogel Column HR3, HR4, and HR6). [c] Functionality.

of the scattering behavior from Porod's law of a two-phase system with finite interface thickness was treated by Koberstein et al.[25]

$$I(Q) = \frac{K_p}{Q^4}\exp(-Q^2\sigma^2) + K_B I_B(Q) \qquad (12)$$

where a Gaussian curve with a standard deviation, σ, was applied to describe the diffusion boundaries. In the Gaussian model for diffusion boundaries, σ can be defined as an interface thickness. The quantities K_B and $I_B(Q)$ represent a proportionality constant and the scattering background due to density fluctuations of labeled and nonlabeled polymers within the interfacial region. The quantity $I_B(Q)$ can be described by many different empirical functions. In this study, the Ornstein−Zernike form was used to fit the scattering background[21]

$$I_B(Q) = \frac{I(0)}{1 + \xi^2(T,\phi)Q^2} \qquad (13)$$

with

$$\xi^2(T,\phi) = \frac{b^2}{36}[\phi_A(1 - \phi_A)(\chi_s - \chi)]^{-1} \qquad (14)$$

where $\xi(T,\phi)$ is the correlation length at temperature T and the fraction of deuterated polystyrene $\phi = \phi_A$, b represents the statistical segment length of styrene, and χ and χ_s are the interaction parameter and interaction parameter at the spinodal point, respectively. The quantity $\xi^2(T,\phi)$ obtained with fully annealed polymer blends of 6% deuterated and 94% protonated polystyrene by fitting methods was found to have a value of 6832 ± 244 Å^2 in the present study.

Direct Nonradiative Energy Transfer Technique (DET)

In DET research, nonradiative energy transfer takes place between a fluorescence donor and an acceptor bonded to separate polymer chains. The fluorescence lifetime of naphthyl groups, the fluorescence donor, is used to measure the diffusion coefficients of polystyrene. The lifetime of excited naphthyl groups decreases in the presence of fluorescence acceptors, anthryl groups, when they are within a distance of a few nanometers. The donor and acceptor are separated in different latex particles at time zero and become mixed as the diffusion of polymer chains proceeds. The area under a donor fluorescence decay curve is a measure of the mixing between donor-labeled and acceptor-labeled polystyrene. The fraction of mixing, $F_m(t)$, at time t provides a measure of the number of polymer chains crossing the interface. Finally, diffusion coefficients were obtained by the Fickian diffusion model. The details of the data analysis can be found elsewhere.[27]

Experimental Section

Materials.[28] Most chemicals except those so identified were purchased from Aldrich and used as received. Polystyrene samples were prepared by Polymer Source, Inc., as described below. Three types of polystyrene with narrow molecular weight distributions were synthesized via anionic polymerization. Purified styrene was added to an initiator solution of secondary butyllithium in tetrahydrofuran (THF) at −78 °C and the polymerization reaction was terminated by adding a few drops of methanol to make polystyrene with hydrogen end groups. The corresponding deuterated polystyrene with H ends was polymerized at room temperature. Polystyrene with one sulfonic acid end group was initiated and propagated by the same method as the H-ended polystyrene and then terminated by adding 1,3-propane sultone. Polystyrene with two sulfonic acid groups was synthesized by using the bifunctional initiator sodium naphthalene, and 1,3-propane sultone as the terminator. The sulfonic acid functionality of the one-ended and two-ended polystyrene was determined by two-phase titration with Hyamine 1622 (Fluka) in water−chloroform using methylene blue as indicator.[29]

The molecular weight and the functionality of the samples are listed in Table 1. The molecular weight of deuterated polystyrenes were measured on gel permeation chromatography instrumentation (Waters Co.) with three columns (Waters Styrogel Columns HR3, HR4, and HR6) under a flow rate of 1.0 mL/min. The molecular weights of these deuterated samples were also measured by small-angle neutron scattering (see Results section), giving similar values with less than 15% difference. For notation, H, P, and S mean H-ended, one-SO_3-ended, and two-SO_3-ended polystyrene, respectively. The temperatures of study, 125, 135, and 145 °C follow the letter designation. Sulfonate chain ends were synthesized by this route, as the corresponding sulfate-chain-ended polymers could not easily be prepared.

Chloromethylation of Polystyrene. Polystyrene as prepared above (1.0 g) was dissolved in chloromethylethyl ether, $ClCH_2OCH_2CH_3$ (10 g), and stirred until the polystyrene was fully dissolved. The $ClCH_2OCH_2CH_3$ was used rather than chloromethylmethyl ether,[30] $ClCH_2OCH_3$, since it is less toxic. To the polystyrene solution was added anhydrous $ZnCl_2$ (0.05 g). The mixture was stirred at room temperature for 30 min. At the end of the reaction, the mixture was precipitated with methanol and then filtered through a glass filter. Filtered polystyrene was dissolved in tetrahydrofuran and again precipitated with methanol. Precipitation was repeated three times to ensure complete removal of zinc chloride. The reaction was checked by proton NMR on a Bruker 360 MHz. The proton peak from $-CH_2Cl$ appears at 4.5 ppm and is integrated to quantify the degree of chloromethylation. The peak at 4.5 ppm indicates the chloromethylation at para-position of phenyl group of polystyrene without any significant side reactions. The quantitative results from proton NMR showed that the degrees of chloromethylation on polystyrene was 0.6 mol %. These fluorescence-labeled polymers were only used for the DET studies.

Reaction between Polystyrene and Fluorescence Groups. To a solution of 9-anthracenemethanol (0.8 g) in dry tetrahydrofuran (10 mL) was added sodium hydride (60%

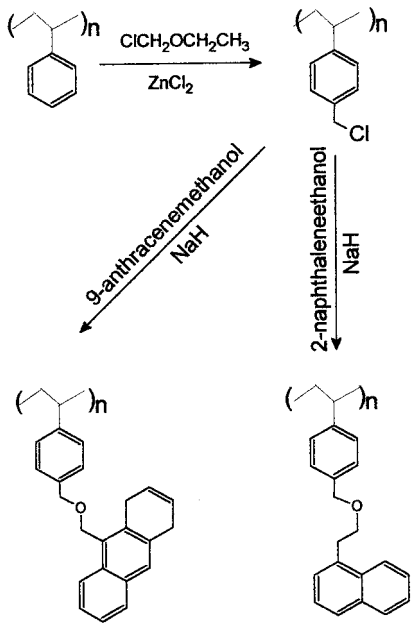

Figure 1. Synthetic route to make fluorescence labeled polystyrene.

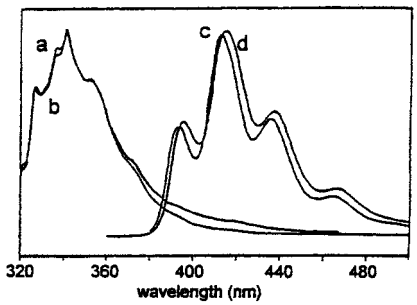

Figure 2. Normalized fluorescence emission spectra of (a) 2-naphthyleethanol, (b) naphthyl-labeled polystyrene, (c) 9-anthracenemethanol, and (d) anthryl-labeled polystyrene. All samples are dissolved in tetrahydrofuran. The naphthyl groups were excited at 280 nm and anthryl groups were excited at 340 nm. Fluorescence spectra show that the emission spectra of free fluorescence groups were almost identical to those attached to polystyrene.

dispersion in mineral oil), and the mixture was stirred at room temperature for 30 min. A solution of chloromethylated polystyrene (0.5 g) in dry tetrahydrofuran (10 mL) was added dropwise, and the reaction mixture was sealed under argon. The sealed mixture in an ampule was stirred and heated to 60 °C for 15−20 h. The reaction mixture was purified by precipitation in methanol (three times). The reaction between 2-naphthyleneethanol and chloromethylated polystyrene was performed with the same method; see Figure 1.

Proton NMR on the Bruker 360 MHz was used to quantify the degree of labeling. The proton NMR peak of CH_2 attached to the anthryl group was shifted to 5.35 ppm from 5.64 ppm (not shown), confirming that the reaction between 9-anthrylmethanol and para-chloromethyl styrene occurred. The peaks at 3.95 and 3.32 ppm which were found in 2-naphthyleneethanol spectrum disappear, and new peaks at 3.70 and 3.43 ppm appear in the reaction product between 2-naphthyleneethanol and *p*-chloromethylstyrene. Both reactions produced higher than 80% yield.

The steady-state fluorescence spectra of labeled polystyrene are seen in Figure 2. Emission fluorescence spectra were obtained to check the labeling of anthryl and naphthyl groups. Naphthyl-labeled polystyrene in tetrahydrofuran was excited at 280 nm and the emission spectra were recorded at room temperature on a Spex Fluorolog II spectrometer. A wavelength of 340 nm was used to excite the anthryl labeled polystyrene. The fluorescence spectrum of naphthyl-labeled polystyrene is almost identical to that of 2-naphthyleneenthanol. The peak of the naphthyl group was observed at 341 nm. The fluorescence spectrum of anthryl-labeled polystyrene is shifted 2.4 nm to longer wavelengths, to 414.6 nm from that of 9-anthracenemethanol, with an almost identical spectral shape.

NMR and fluorescence emission spectra show that the labeling was successful and the characteristics of the fluorescence groups on the polystyrene are identical to those of the unbound fluorescence groups, ensuring that the labeled samples are appropriate for fluorescence studies.

Latex Preparation. An artificial miniemulsification[31] process was used to prepare latices with uniform particle sizes in the presence of sodium lauryl sulfate and long chain alcohols as surfactant and cosurfactants, respectively. A polymer dispersion is created by ultrasonification and filtration of the water/polymer mixture through a uniform pore size membrane (0.4 μm polycarbonate membrane, Nuclepore). Particle sizes by transmission electron microscopy are 100−120 nm, with a polydispersity of less than 1.3. After solvent was removed by distillation, a fluorescent donor-labeled latex was blended with an acceptor-labeled latex. The two-latex mixture was dried at 50 °C for 1 day, followed by surfactant and cosurfactant removal in a Soxhlet apparatus with methanol, and then distilled deionized water. Residual surfactant and cosurfactant contents were monitored by GPC and DSC. A differential scanning calorimeter (DSC, TA Co.) was used to check the T_g of purified samples under nitrogen atmosphere at a heating rate of 10 °C/min. The T_g values of H-end polystyrene (H), one-SO_3-end polystyrene (P), and two-SO_3-end polystyrene (S) were found to be 108.4, 108.3, and 108.7 °C at the midpoint of the transition region, respectively, indicating that all samples were purified and behaving substantially identically in this regard.

The original polystyrene from the anionic polymerization has sulfonate end groups in acid form. After miniemulsification the sulfonate groups presumably are neutralized by Na^+ since a large quantity of sodium is provided by the sodium lauryl sulfate. The washing process may remove most of the sodium as well as the surfactant. However, the interaction between sodium and sulfonate groups is so strong that some sulfonate groups may remain neutralized even after the washing. To check the degree of neutralization of sulfonate groups, the amount of sodium in the polystyrene sample was measured (Galbraith Laboratories Inc.). Polystyrene with two sulfonate ends has 59% of its sulfonate groups in neutralized form.

In another experiment, the presence of ionic groups on the surface of the latex particles was measured by a conductance method.[32] Surfactants, including sodium lauryl sulfate, and the counterions were removed by a mixed ion-exchange resin to produce the acid form. The cleaned latex dispersion was titrated by a 0.02 N NaOH water solution, while the conductance was monitored.[33] The titration results of ionic groups at the cleaned latex surface shows that essentially 100% of sulfonate end groups were located on the latex surface with an error of ±10%.

Sintering and Film Annealing. A dried latex mixture was compressed under 10 MPa of pressure at 100−110 °C for 30 min to 1 h. These conditions were chosen to produce a transparent film with a minimum interdiffusion between latex particles.[14] Sample disks with a 1.3 cm diameter and a 0.4 mm thickness were clamped between glass slides to inhibit distortion, and were annealed at 115−140 °C. The actual temperature of the samples was directly measured by a thermocouple in contact with the sample surface. Five to seven minutes were usually needed to reach the desired annealing temperature. All times reported are times in the mold and are ±2 min due to thermal lag of heating. The temperatures reported all range ±1.0 °C based on previous studies.

SANS Measurements. The SANS experiments were carried out at the National Institute of Standards and Technology, NIST, in Gaithersburg, MD. The wavelength of the incident beam was monochromatized to 20 Å by a velocity selector with $\Delta\lambda/\lambda = 0.25$. The observed scattering intensity was corrected for electronic noise, background radiation, and detector inho-

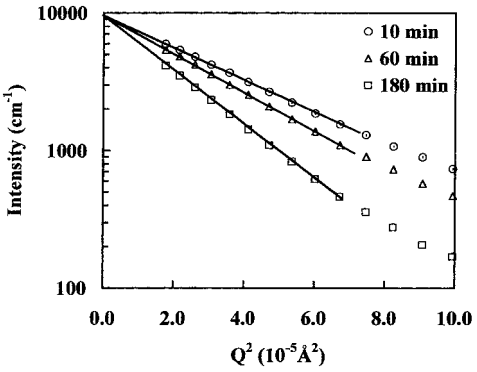

Figure 3. Determination of the radius of deuterated polystyrene via Guinier plots.

mogeneity. It was normalized against a polymer standard to give the absolute intensity. Finally, it was circularly averaged to obtain the scattering intensity as a function of the wave vector, Q. Disk specimens of 0.52 mm thickness and 15 mm diameter were used throughout the measurements. Samples on masks of 12.5 mm in diameter were separated from the source by a distance 4.1 m. The sample-to-detector distance was 3.6 m. A two-dimensional position sensitive detector (128 × 128 cm^2 with 1 cm resolution) was used. The SANS data were collected over the range of scattering vectors 0.004 Å^{-1} ≤ Q ≤ 0.039 Å^{-1}. The recorded intensities for the samples and blanks were radially averaged and converted to absolute values. Data were reduced and standard deviations were calculated as described elsewhere.[34] Fits were made with linear or nonlinear least squares and are plotted with error bars of 1 standard deviation. In figures where the error bars were smaller than the plotted points, the bars were omitted for clarity.

DET Measurements. The lifetime of naphthyl groups was measured on a 199-Florescence spectrometer (Edinburgh Instruments Ltd.). A pulsed hydrogen flash lamp selectively excites the naphthalene fluorophore at 280 nm. The emission is detected at 340 nm via a photomultiplier tube operating in a time-correlated single-photon-counting mode. Further details regarding the instrument setup were reported elsewhere.[35] The raw data were first deconvoluted from the instrument response function, which typically has a 2−4 ns width at half-height. Many functions could be applied to an analysis of the decay curve, however, a double-exponential function built into the instrument software was used which produced reasonable χ^2 values (≤1.3).

Results

It should be noted that all diffusion coefficients at short-times, namely less than the reptation time of a polymer chain, are *apparent* diffusion coefficients. The apparent diffusion coefficients can be obtained, based on a Fickian diffusion model. Arguably, a Fickian diffusion model might not be valid for polymer interdiffusion at short-times. However, the Fickian model seems to be the best model up until now to describe the interdiffusion process in latex films.

SANS Results. Diffusion Coefficient Measurements by Guinier Plots. Guinier plots in Figure 3 were prepared to determine the radius of gyration of the particles in films annealed at 135 °C, showing that the scattering intensity decreases at higher angles as annealing time increases. On the basis of the linear lines (Q range of 0.00421 ≤ Q ≤ 0.0082) the radii of gyration were determined (Table 2). The radius of gyration of the sintered particles is larger than that of samples annealed for very short times due to the deformation of the particles after the high-pressure sintering process (data not shown). The particle deformation is believed to be significantly lost by physical relaxation after a short period of annealing. The nonequilibrium state of polymer chain conformations and the Rouse relaxation between entanglements (i.e., rubber elasticity effects) may allow for the fast physical relaxation.[36] The apparent expansion of the particle size can be observed after a short period of annealing.

Table 2. Radius of Gyration (Å) of Polystyrene Samples Annealed at 135 °C

annealing time (min)	H end	one SO_3 end	two SO_3 end
0	285.4 ± 1.1		
10	286.6 ± 0.7	276.2 ± 0.9	276.2 ± 1.9
20	293.6 ± 1.6		279.6 ± 2.0
40		282.5 ± 0.9	
50	308.4 ± 1.3		286.5 ± 1.3
60	312.0 ± 1.4	289.1 ± 1.2	286.6 ± 0.9
120	337.2 ± 1.0	299.7 ± 1.0	294.0 ± 1.5
180	366.1 ± 0.9	300.4 ± 1.1	309.9 ± 1.1
240	376.1 ± 1.0		307.4 ± 1.3
300		309.9 ± 0.5	
540	396.8 ± 1.2		
600			323.8 ± 1.1
720		324.4 ± 0.8	
81200			356.1 ± 1.6
1320		337.9 ± 0.1	
1800			389.5 ± 2.8
3120			420.8 ± 5.4

Table 3. Diffusion Coefficients (10^{-16} cm^2/S) of Polystyrene Samples Annealed at 135 °C

annealing time (min)	H end	one SO_3 end	two SO_3 end
20	1.126 ± 0.378		0.521 ± 0.244
40		0.326 ± 0.056	0.405 ± 0.050
50	0.899 ± 0.077		
60	0.844 ± 0.061	0.405 ± 0.039	0.327 ± 0.040
120	0.797 ± 0.025	0.342 ± 0.014	0.256 ± 0.010
180	0.847 ± 0.017	0.228 ± 0.007	0.316 ± 0.007
240	0.716 ± 0.011		0.220 ± 0.003
300		0.189 ± 0.004	
540	0.395 ± 0.004		
600			0.134 ± 0.003
720		0.113 ± 0.001	
1200			0.118 ± 0.003
1320		0.080 ± 0.001	
1800			0.117 ± 0.003
3120			0.090 ± 0.002

The diffusion coefficients can be obtained by eq 9 or 10. The two equations yield identical diffusion coefficients since both equations are based on the identical assumptions of a Fickian model and the scattering equation.[24] The diffusion coefficients in Table 3 show that H-ended polystyrene has higher diffusion coefficients than one-sulfonate-ended and two-sulfonate-ended polystyrene.

Temperature Dependence of Diffusion. To investigate the temperature effect on interdiffusion, H-ended, one-sulfonate-ended, and two-sulfonate-ended polystyrenes were annealed at 125, 135, and 145 °C. The average diffusion coefficient at a given temperature was determined by a linear regression based on eq 10. In Figure 4, the activation energies for H-ended, one-sulfonate-ended, and two-sulfonate-ended polystyrenes were obtained by using the Arrhenius equation. Activation energies for H-ended, one-sulfonate-ended, and two-sulfonate-ended polystyrenes were 63 ± 2.5, 68 ± 4.8, and 71 ± 13 kcal/mol, respectively. Although the absolute values of diffusion coefficients for the three types of polystyrene are different, the activation energies are similar. These activation energies indicate that

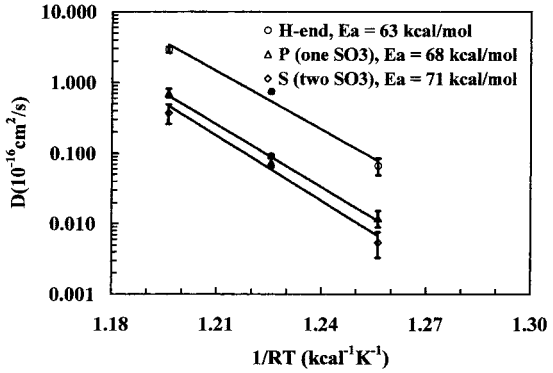

Figure 4. Arrhenius plots to determine the activation energies of polystyrene with H ends (circles), one sulfonate end (triangles), and two sulfonate ends (diamonds).

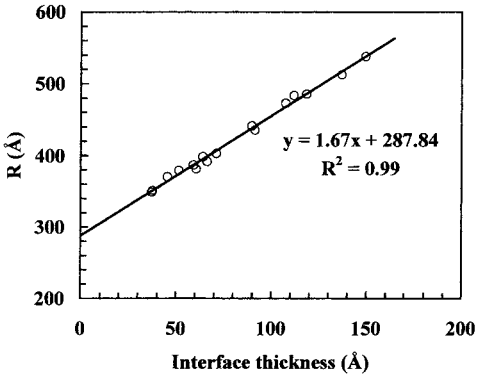

Figure 5. Apparent particle radius vs interface thickness via Porod plots.

the same diffusion mechanism governs the diffusion process of the three types of polystyrene. According to the WLF equation, the diffusion coefficient is a function of free volume, which depends on the difference between annealing temperature and T_g. The differences in T_g of the three types of polystyrene are identical within experimental error. The T_g data above combined with the activation energy data indicate that the sulfonate end groups do not change the diffusion mechanism, only changing the absolute values of diffusion coefficients.

The Interpenetration Depth vs Interface Thickness. The latex particle diameter was chosen as the initial particle size as in previous studies.[14,16] However, the initial particle size in the film should be different from the latex particle size because of particle deformation during film preparation. To estimate the initial particle size, a new approach was used, assuming that the interpenetration depth defined by eq 7 is proportional to the interface thickness determined by the Porod plot in eq 12. The interface thickness, σ, can be determined for a given SANS spectrum while the interpenetration depth, d, requires an initial particle size, R_o

$$d = (R(t) - R_o) = a\sigma(t) \qquad (15)$$

where a represents a proportionality constant.

A linear regression of $R(t)$ against $\sigma(t)$ of H-ended polystyrene was performed to obtain the proportionality constant and R_o in Figure 5. The regression result shows that the interpenetration depth is 1.67 times larger than the interface thickness by the Porod plot. The quantities R_o for H-end, one-SO_3-end, and two-SO_3-end samples are listed in Table 4.

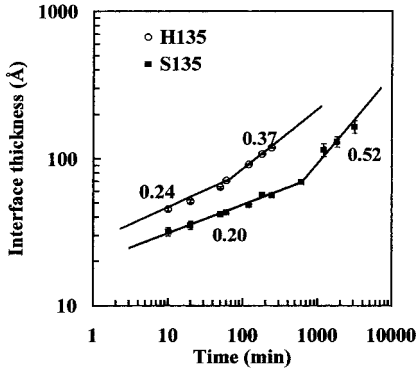

Figure 6. Scaling law time dependence for interfacial thickness during annealing of latex films. H-ended (circles, H135) and two-SO_3-ended (rectangles, S135) polystyrene annealed at 135 °C.

Table 4. Linear Regression Results to Obtain the Initial Particle Size and the Proportionality Constant *a* in Eq 15

designation	samples	R_o (Å)	a
H	H end	287.8 ± 3.3	1.68 ±0.038
P	one SO_3 end	294.6 ± 4.4	1.71 ±0.079
S	two SO_3 end	323.9 ± 5.6	1.37 ±0.076

Even though the two quantities, interpenetration depth and interface thickness, are basically the same measure of the diffusion distance as shown above, the interface thickness has an advantage in expressing the diffusion distance since it does not require the assumption of the ambiguous quantity, initial particle size.

Diffusion Distance vs Time. Figure 6 shows the time dependence of the interface thickness. The data approximately follow the $d(t) \sim t^{1/4}$ relationship predicted for the short-time regime, which changes over to $d(t) \sim t^{1/2}$ at the long-time regime. The slopes show breaks at close to the theoretical reptation time[37] of $T_r = R_e^2/3\pi^2 D$, where R_e represents the chain end-to-end distance. However, the interface thickness at the break point is about $0.4R_g$, lower than the classical value of $0.8R_g$. Thus, the present work confirms that the classical relaxation time is correct, but the distance diffused is one-half that of the classical value.

Kim et al.[16] reported that the interpenetration distance from the interface at the reptation time is about $0.4R_g$, also lower than the theoretical value[12] of $0.8R_g$. However, a quantitative explanation for the lower diffusion distance was not available. Welp et al.[36] independently confirmed Kim's result by experiment and theory. Their specular neutron reflectivity experiments on deuterium-labeled polystyrene in either the central 50% of the polymer or in the two end sections (25% each) showed that the average monomer interpenetration distance, $\langle X \rangle$, at reptation time is $0.4R_g$. They pointed out that the experimental quantity $\langle X \rangle$ differs from the actual diffusion distance X since $\langle X \rangle$ is a measure of the distance from the interface plane rather than the true diffusion distance.

Figure 7 depicts the difference between true diffusion distance, X, and the measured diffusion distance $\langle X \rangle$ from the interface. In the case that the experiment monitors only polymer segments moving across the interface, the measured diffusion distance, $\langle X \rangle$, should equal $0.5X$. Hence, the measured diffusion distance equals $0.4\ R_g$, half of de Gennes's prediction of $0.8\ R_g$. This relationship between the true diffusion distance and the measured diffusion distance holds only for the

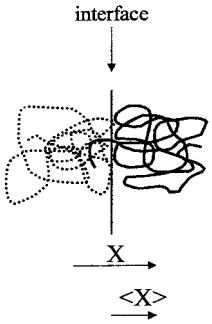

Figure 7. Schematic diagram to explain the difference between true diffusion distance, X, and measured diffusion distance from the interface $\langle X \rangle$. Dotted line and solid line represent a polymer chain at time zero and time t, respectively.

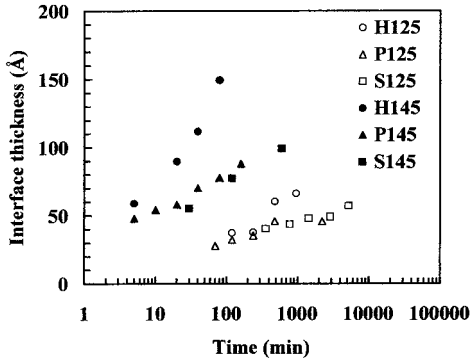

Figure 8. Interface thickness via the Porod plots of H-ended (circles, H125, H145), one-SO_3-ended (triangles, P125, P145), and two-SO_3-ended polystyrene (rectangles, S125, S145).

Table 5. Time Dependence of Interpenetration Depth: Slope of the log(interpenetration depth) − log(time)

designation	sample (annealing temperature (°C))	reptation time (T_r) (min)	exponent value $t < T_r$	exponent value $t > T_r$
H125	H ends (125)	1250	0.29 ± 0.07	
H135	H ends (135)	205	0.23 ± 0.03	0.43 ± 0.09
H145	H ends (145)	28	0.31 ± 0.03	
P125	one SO_3 end (125)	6750	0.10 ± 0.02	
P135	one SO_3 end (135)	1051	0.17 ± 0.01	
P145	one SO_3 end (145)	114	0.21 ± 0.01	
S125	two SO_3 ends (125)	15400	0.13 ± 0.02	
S135	two SO_3 ends (135)	921	0.27 ± 0.02	0.53 ± 0.04
S145	two SO_3 ends (145)	225	0.22 ± 0.01	

short time regime, roughly less than reptation time. At longer time scales, the measured diffusion distance becomes closer to the true diffusion distance.

The interface thickness of the latex film at time zero is nearly zero but exceeds 27 Å as soon as the film is annealed, regardless of the annealing temperature. This initial "bursting" phenomenon was observed in other polymer diffusion experiments.[16,36,38,39] The nonequilibrium polymer conformation at the interface, surface tension between the polymer layers, and the Rouse relaxation between entanglements are proposed as the origin of the initial "bursting." The dominant mechanism of the "bursting" phenomenon is not understood yet.

Table 5 shows the slope of log(d) vs log(time). Most experimental data were obtained in the short-time regime, before the reptation time, giving d considerably smaller than R_g. The time dependence of the interpenetration depth, d, is similar to that of interface thickness σ via the Porod plot. Figure 8 shows that the interface thickness of H-ended polystyrene is larger than that of the one-SO_3-ended and two-SO_3-ended polystyrenes at a given time and annealing temperature.

Table 6. Apparent Molecular Weight and Radius of Gyration of Fully Annealed Samples[a]

designation	deuterated/protonated	M_w	R_g (Å)	$R_g/M_w^{0.5}$
d-H/h-H	H ends/H ends	317 800	161 ± 5	0.285
d-P/h-P	one SO_3 end/one SO_3 end	238 300	134 ± 3	0.275
d-P/h-H	one SO_3 end/H ends	350 500	163 ± 3	0.275
d-S/h-S	two SO_3 ends/two SO_3 ends	247 500	139 ± 2	0.280
d-S/h-H	two SO_3 ends/H ends	1 447 500	331 ± 23	0.271

[a] Samples consist of 6% deuterated and 94% protonated polystyrene.

Aggregation. The polystyrene aggregate structure in the fully annealed state was investigated since the ionic end groups can induce an ionomer aggregation structure. Register et al.[40] investigated the ionic aggregation of telechelic polystyrene with carboxyl end groups. Na^+-neutralized carboxyl end groups lead to an "ionomer peak" with small-angle X-ray scattering (SAXS), indicating ionic aggregation while polystyrene with ester end groups does not show the "ionomer peak". However, no interphase scattering was visible in SANS data of polystyrene with Na^+-neutralized carboxyl end groups because the ion−polymer neutron scattering contrast is much lower than the corresponding X-ray contrast.

To investigate the polystyrene aggregate structure, various samples were prepared. Since a mixture of the same type of deuterated and protonated polystyrene does not show polystyrene aggregation,[40] a mixture between polystyrene with sulfonate ends and polystyrene with H ends was prepared. If aggregation due to the end groups exists, the apparent molecular weight should be higher than observed with single molecules.

The apparent molecular weight and radius of gyration were determined on fully annealed samples by a Zimm plot

$$I^{-1} = \frac{1}{C_N M_w}\left(1 + \frac{Q^2 R_g^{\,2}}{3} + ...\right) \qquad (16)$$

where M_w represents the weight-average molecular mass and C_N is a calibration constant given by

$$C_N = \frac{(a_H - a_D)^2 N_a \rho (1 - X) X}{M_p^{\,2}} \qquad (17)$$

where a_H and a_D are the scattering length of a protonated and deuterated structural unit, ρ and X represent the density of the polymer and the mole fraction of the labeled chains, and N_a and M_p represent Avogadro's number and the mer molecular weight, respectively.

From the SANS spectra of fully annealed samples, the molecular weight and the radius of gyration of the chains and/or aggregates were determined. The sulfonate end groups of the samples were not neutralized but were used as received in the acid form. The mixture of deuterated and protonated polystyrene of the same end groups shows a molecular weight smaller than GPC data with the quantity $R_g^2/M_w^{1/2}$ close to the reported value, 0.275 (Table 6).[41] However, the mixture of different types produced higher molecular weights. Deuterated one-SO_3-ended polystyrene in protonated H-ended polystyrene has a molecular weight 1.5 times higher than that in the same type of polystyrene. Deuterated two-SO_3-end polystyrene in protonated H-

Table 7. Equilibrium Constants for Sulfonate End Group Aggregation[a]

sample designation	average no. of aggregates, N (SANS)	tot. sulfonate end groups (mol/L)	free[b] [$-SO_3H$] (mol/L)	aggregate [SO_3H••SO_3H] (mol/L)	equilib const
d-P/h-H	1.47	1.9×10^{-4}	7.0×10^{-5}	6.2×10^{-5}	1300
d-S/h-H	5.85	3.9×10^{-4}	1.3×10^{-4}	1.3×10^{-4}	730

[a] Samples consist of 6% deuterated and 94% protonated polystyrene. [b] For one-sulfonate-end polystyrene(d-P/h-H): N = [total sulfonate end groups]/([$-SO_3H$] + [SO_3H••SO_3H]). For two-sulfonate-end polystyrene(d-P/h-H): N = [total sulfonate end groups]/([$-SO_3H$]/2)

end polystyrene has an even higher molecular weight, 5.8 times, while maintaining a value of $(R_g^2/M_w)^{1/2}$ within statistical error of 0.275, the single chain value.

The higher molecular weight of one-SO_3-ended polystyrene and two-SO_3-end polystyrene in protonated H-ended polystyrene indicates that the end groups induce polystyrene aggregation. The aggregation cannot be observed in the all sulfonate mixture due to the random interaction between protonated and deuterated species. By contrast, polystyrene with sulfonate end groups in H-ended polystyrene tend to be aggregated if there is any preferable interaction between the sulfonate groups over styrene mers or over H-end groups. The hydrogen bond between the sulfonate groups should be the origin of the aggregate since the sulfonate groups is not neutralized. The equilibrium constant and H-bond energy can be estimated based by the following equation and the SANS data.

$$PS{-}SO_3H + PS{-}SO_3H \leftrightarrow PS{-}SO_3H{\cdots}SO_3H{-}PS$$

$$\Delta G = -RT \ln K_{eq} = -RT \ln([PS{-}SO_3H{\cdots}SO_3H{-}PS]/[PS{-}SO_3H]^2) \quad (18)$$

where ΔG and K_{eq} represent the Gibbs free energy and the equilibrium constant between polystyrene and its dimer, respectively.

Here it is assumed that only linear chains are formed from end-to-end aggregation and no star-shape polymers are formed. This assumption is based on the observation of $(R_g^2/M_w)^{1/2} = 0.275$ for all polymer samples in Table 6.

The concentration of sulfonate end groups and the average number of aggregates of deuterated one-sulfonate-ended polystyrene and protonated H-ended polystyrene are listed in Table 7, resulting in $\Delta G = -8.0$ kcal/mol which is on the order of one or two hydrogen bonds. For the mixture of deuterated two-sulfonate ended polystyrene and protonated H-ended polystyrene,[42] ΔG was found to be -7.5 kcal/mol, substantially identical to that of the one-sulfonate-ended polystyrene case.

The latex films used for the diffusion studies may have different free energies since the sulfonate groups were partly neutralized by salts since the purification process of the latex is based on a water and methanol extraction method, primarily designed to remove surfactants and cosurfactants. In fact, 59% of the sulfonate was neutralized by sodium as described in the Experimental Section. The strong interaction between sulfonate and salt, mainly sodium, may conserve the neutralized state of sulfonate even after the extraction process. The aggregation number in the neutralized sulfonate depends on salt and sulfonate concentration as many ionomer studies have revealed.

DET Experiments. Since a previous study by DET experiments[43] shows that polystyrene of $M_n = 100\,000$ with H ends has a lower diffusion coefficient than

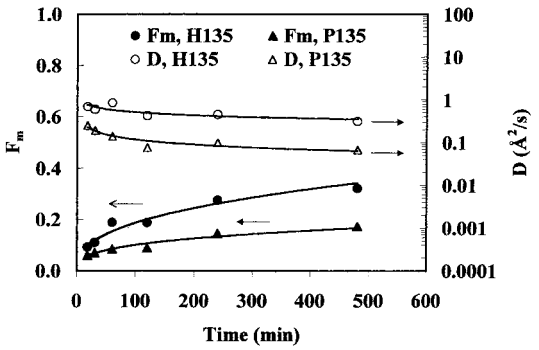

Figure 9. Diffusion coefficients and the fraction of mixing of polystyrene with H ends and one SO_3 end as monitored by DET. The curves represent the fraction of mixing of H end (F_m, H135) and one SO_3 end (F_m, P135), and the diffusion coefficient of H ends (D, H135) and one SO_3 end (D, P135).

Table 8. DET Measurement of Diffusion Coefficients (10^{-16} cm²/S) of Polystyrene Samples Annealed at 135 °C

annealing time (min)	D (H end) (H135)	D (one SO_3 end) (P135)
18	0.69	0.25
30	0.59	0.19
60	0.85	0.14
120	0.42	0.076
240	0.45	0.098
480	0.31	0.068

polystyrene with one sulfate end group, a comparison between DET and SANS was performed. The purpose of the DET experiment in this study was to compare SANS and DET to ensure that neither method produces instrumental artifacts. Polystyrene samples from the SANS experiments were labeled with fluorescence groups to be used for the DET experiments as described above. Figure 9 shows a comparison of the fraction of mixing and the diffusion coefficients between the polystyrene with one-SO_3-end and two H ends. DET confirms that H-end polystyrene has higher diffusion coefficients than one-SO_3-ended polystyrene (Table 8). Therefore, the discrepancy of the previous study by DET and the present SANS study should originate from factors other than the instrumental artifacts. Possible sources of the discrepancy are the difference in the nature of end groups (sulfonate vs sulfate),[43] the molecular weight or its polydispersity, and/or the aggregate structure described in the next section.

Discussion

Diffusion Model for Polystyrene with Ionic Groups at Interfaces. The model below is designed to answer two questions: (1) why the present SANS results show lower D for one sulfonate end while the previous DET study[43] shows higher D for one sulfate end; (2) why the D values of one sulfonate end and two sulfonate end are similar while the D of H ends is much higher than those with sulfonate ends.

The diffusion process starting at the polymer latex interface may be controlled by two opposing factors,

namely surface segregation of end groups and aggregation of the end groups. The surface segregation of end groups increases the initial diffusion coefficient of a polymer chain[43] while the aggregation of end groups decreases it.

The ionic end groups are preferentially located at the latex surface in the dispersion and surface segregation of end groups probably continues to exist in the film at the outset of interdiffusion.

One-Sulfonate-Ended Chains. The present model to describe the sulfonate end group effect on interdiffusion assumes that they form temporary aggregates. One possibility is that the temporary aggregates may form "pseudo" star−polymer structures,[44−47] The number of arms in an aggregate should depend on the characteristics of end groups. The quantity $R_g/M^{0.5}$ in Table 6 indicates that the acid form of sulfonate end groups induces a two-arm star polymer.

A polymer chain continues to diffuse while it forms a reversible aggregate with other polymer chains. The average diffusion coefficients depend on the number of chains in the aggregate.

The slow effect of diffusion coefficients due to the aggregation of the sulfonate-end groups becomes larger with higher molecular weight due to the slower motion of the chains. Since the molecular weight of the polymers in the present SANS study is higher than that of the previous DET study[43] by a factor of 3−5, the slow effect due to the end groups should play a more important role in the present system.

Two Sulfonate-End Chains. The number of polymer chains in an aggregate may be higher for the two sulfonate ended polystyrene than one-sulfonate-ended polystyrene since the sulfonate concentration of two-sulfonate-ended polystyrene in the bulk is 2 times higher than that of one-sulfonate-ended polystyrene. The higher number of arms of such pseudo-star polymers can cause the slower diffusion rates. However, the diffusion coefficient for a higher number of arms (>3) does not decrease as predicted.[46,47]

Noting $(R_g^2/M_w)^{1/2}$ (Table 6) remains constant, a better modeling might be end-to-end aggregation, creating temporary chains several times that of the primary chain. While a mix of all of the above is possible, a firm conclusion for the leading cause of the lower diffusion coefficients will have to await further experiments.

Conclusions

The interdiffusion behavior of polystyrene with H ends, one sulfonate end, and two sulfonate ends was investigated with small-angle neutron scattering (SANS) and a direct nonradiative energy transfer technique (DET). High molecular weight ($M_n \cong 300\,000$) polystyrene was confined in latex particles via an artificial miniemulsification technique and interdiffusion of polystyrene in latex films was permitted at temperatures above T_g. At annealing temperatures of 125−145 °C (Figure 4) the diffusion coefficients of polystyrene with H ends were, on average, 5 and 10 times higher than that of polystyrene with one sulfonate end and two sulfonate ends, respectively. The sulfonate end group effects on the diffusion coefficients are interpreted as the competition between diffusion enhancement by the surface segregation of the end groups and diffusion reduction by end group aggregation.

Acknowledgment. The authors would like to acknowledge financial support through National Science Foundation Grant No. CTS-9810703.

References and Notes

(1) Klein, J. *Science* **1990**, *250*, 640.
(2) Hunt, M. O.; Belu, A.; Linton, R.; DeSimone, J. M. *Macromolecules* **1993**, *26*, 4854.
(3) Affrossman, S.; Hartshorne, M.; Kiff, T.; Pehtrick, R. A.; Richards, R. W. *Macromolecules* **1994**, *27*, 5341.
(4) Schaub, T. F.; Kellogg, G. J.; Mayes, A. M.; Kulasekere, R.; Ankner, J. F.; Kaiser, H. *Macromolecules* **1996**, *29*, 3982.
(5) Botelho de Rego, A. M.; Lopes da Silva, J. D.; Vilar, M. R.; Schott, M.; Petijean, S.; Jerome, R. *Macromolecules* **1993**, *26*, 4986.
(6) Elman, J. F.; Johs, B. D.; Long, T. E.; Koberstein, J. T. *Macromolecules* **1994**, *27*, 5341.
(7) Schmidt, I.; Binder, K. *J. Phys (Paris)* **1985**, *46*, 1631.
(8) Jones, R. A. L.; Kramer, E. J. *Polymer* **1993**, *34*, 115.
(9) Reiter, J.; Zifferer, G.; Olaj, O. F. *Macromolecules* **1990**, *23*, 224.
(10) Cifra, P.; Nies, G.; Karasz, F. E. *Macromolecules* **1994**, *27*, 1166.
(11) Jalbert, C.; Koberstein, J. T.; Hariharan, A.; Kumar, S. K. *Macromolecules* **1997**, *30*, 4481.
(12) Wool, R. P. *Polymer Interfaces*; Hanser Publisher: New York, 1995.
(13) Blackley, D. C. *Emulsion Polymerisation*; Applied Science Publishers: Ltd.: London, 1975; p 172.
(14) Yoo, J. N.; Sperling, L. H.; Glinka, C. J.; Klein, A. *Macromolecules* **1991**, *24*, 2868.
(15) Yoo, J. N.; Sperling, L. H.; Glinka, C. J.; Klein, A. *Macromolecules* **1990**, *23*, 3962.
(16) Kim, K. D.; Sperling, L. H.; Klein, A.; Hammouda, B. *Macromolecules* **1994**, *27*, 6841.
(17) Kim, H.-B.; Winnik, M. A. *Macromolecules* **1994**, *27*, 1007.
(18) Hansch, H. H.; Petrovska, D.; Landel, R. F.; Monnerie, L. *Polym. Eng. Sci.* **1987**, *27*, 149.
(19) Kline, D. B.; Wool, R. P. *Polym. Eng. Sci.* **1988**, *28*, 52.
(20) de Gennes, P. G. *J. Chem. Phys.* **1971**, *55*, 572.
(21) de Gennes, P. G. *Macromolecules* **1976**, *4*, 587.
(22) Kim, Y. H.; Wool, R. P. *Macromolecules* **1983**, *16*, 1115.
(23) Summerfield, P. G.; Ullman, R. *Macromolecules* **1987**, *20*, 401.
(24) Eu, M.-D.; Ullman, R. *Film Formation in Waterborne Coatings*, American Chemical Society: Washington, DC, 1996.
(25) Koberstein, J. T.; Morra, B.; Stein, R. S. *J. Appl. Crystallogr.* **1980**, *13*, 34 and references therein.
(26) Han, C. C.; Bauer, B. J.; Clark, B. J.; Muroga, Y.; Matsushita, Y.; Okada, M.; Tran-cong, Q.; Chang, T.; Sanchez, I. *Polymer* **1988**, *29*, 2002.
(27) Tamai, T.; Pineng, P.; Winnik, M. A. *Macromolecules* **1999**, *32*, 6102.
(28) Certain commercial materials and equipment are identified in this paper in order to specify adequately the experimental procedure. In no case does such identification imply recommendation by the National Institute of Standards and Technology nor does it imply that the material or equipment identified is necessarily the best available for this purpose.
(29) Quirk, R. P.; Kim, J. *Macromolecules* **1991**, *24*, 4515.
(30) Jones, G. D. *Ind. Eng. Chem.* **1952**, *44*, 2686.
(31) Mohammadi, N.; Kim, K. D.; Sperling, L. H.; Klein, A. *J. Colloid Interface Sci.* **1993**, *157*, 124.
(32) Jayasuriya, R. M.; El-Aasser, M. S.; Vanderhoff, J. W.; Yue, H. J. *J. Polym. Sci., Polym. Chem. Ed.* **1985**, *23*, 2819.
(33) Jayasuriya, R. M.; El-Aasser, M. S.; Vanderhoff, J. W.; Yue, H. J. *J. Polym. Sci., Polym. Chem. Ed.* **1985**, *23*, 2819.
(34) *NG3 and NG7 30-meter SANS Instruments Data Acquisition Manual*; National Institute of Standards and Technology Cold Neutron Research Facility: Gaithersburg, MD, 1996.
(35) Boczar, E. M.; Dionne, B. C.; Fu, Z.; Kirk, A. B.; Lesko, P. M.; Koller, A. D. *Macromolecules* **1993**, *26*, 5772.
(36) Welp, K. A.; Wool, R. P.; Agrawal, G.; Satija, S. K.; Pispas, S.; Mays, J. *Macromolecules* **1999**, *32*, 5127.
(37) Whitlow, S. J.; Wool, R. P.; *Macromolecules* **1991**, *24*, 5926.
(38) Karim, A.; Mansour, A.; Felcher, G. P.; Russell, T. P. *Phys. Rev. B* **1990**, *42*, 6848.
(39) Stamm, M.; Huttenbach, S.; Reiter, G.; Springer, T. *Europhys. Lett.* **1991**, *14*, 451.
(40) Register, R. A.; Cooper, S. L.; Thiyagarajan, P.; Chakatapani, S.; Jerome, R. *Macromolecules* **1990**, *23*, 2978.

(41) Cotton, J. P.; Decker, D.; Benoit, H.; Farnoux, B.; Higgins, J.; Jannink, G.; Ober, R.; Picot, C.; desCloizeaux, J. *Macromolecules* **1974**, *7*, 863.
(42) Since polymer chains are assumed to be linearly connected, the number of end group in aggregate state and free state can be calculated. For example, when the average number of aggregate is 6, there are 12 sulfonate end groups in an aggregate that consists of 10 end groups in the aggregate and 2 in the free state.
(43) Kim, S. D.; Boczar, E. M.; Klein, A.; Sperling, L. H. *Langmuir*, in press.
(44) de Gennes, P. G. *J. Phys.* **1975**, *36*, 1199.
(45) Klein, J.; Fletcher, D.; Fetters, L. J. *Nature* **1983**, *304*, 526.
(46) Antonietti, M.; Sillescue, H. *Macromolecules* **1986**, *19*, 798.
(47) Shull, K. R.; Kramer, E. J.; Fetters, L. J. *Nature* **1990**, *345*, 28.

MA000432U